Neuroradiology (2001) 43: 1023–1030
DOI 10.1007/s002340100629

S. Nagamachi
S. Jinnouchi
K. Nabeshima
R. Nishii
L. Flores II
T. Kodama
K. Kawai
S. Tamura
K. Yokogami
T. Samejima
S. Wakisaka

The correlation between ^{99m}Tc-MIBI uptake and MIB-1 as a nuclear proliferation marker in glioma – a comparative study with ^{201}Tl

Received: 14 November 2000
Accepted: 14 April 2001
Published online: 13 July 2001

S. Nagamachi (✉) · S. Jinnouchi · R. Nishii · L. Flores II · T. Kodama · S. Tamura
Department of Radiology,
Miyazaki Medical College,
Miyazaki 889-1692, Japan
E-mail:
snagama@post1.miyazaki-med.ac.jp
Phone: +81-985-851510ext.2244
Fax: +81-985-857172

K. Nabeshima
Department of Pathology,
Miyazaki Medical College Hospital,
Miyazaki 889-1692, Japan

K. Yokogami · T. Samejima · S. Wakisaka
Department of Neurosurgery,
Miyazaki Medical College,
Miyazaki 889-1692, Japan

K. Kawai
Central Research Laboratories,
Miyazaki Medical College,
Miyazaki 889-1692, Japan

Abstract Technetium-99m methoxy-isobutylisonitrile (MIBI), like thallium-201 (^{201}Tl), is a highly efficient agent for the diagnosis and monitoring of glioma tumors. Although ^{201}Tl uptake is known to be partly associated with proliferative activity, little is known about the correlation between MIBI uptake and proliferation activity in gliomas. The current study was performed to assess the correlation between MIBI uptake and proliferative activities in gliomas, estimated by the monoclonal antibody to Ki-67 antigen (MIB-1) staining method. By comparing the results with those of ^{201}Tl, we determined which tracer would be suitable for estimating proliferative activities. Twenty-four presurgical glioma patients (six with low-grade gliomas, five with anaplastic astrocytomas, and 13 with glioblastomas) were given MIBI and ^{201}Tl SPECT. Early (10 min after injection) and delayed images (3 h after injection) were obtained for both MIBI and ^{201}Tl scintigraphy. SPECT parameters, early ratio (ER), delayed ratio (DR), and retention index (RI) were obtained in both radiopharmaceuticals. All patients underwent subsequent surgical excision, and the specimens were immunostained for MIB-1. The proliferative activity was measured as a percentage positive nuclear area for MIB-1 (MI; MIB-1 index). To evaluate the relationship between the proliferative activity and SPECT parameters, we performed a correlation analysis. MI correlated with the MIBI uptake ratio (r = 0.75 for ER, and r = 0.7 for DR). Both DR and RI of ^{201}Tl also correlated with MI, but weakly (r = 0.6 for DR, and r = 0.59 for RI). There was no significant correlation between the MIB-1 index and the other parameters. MIBI-uptake parameters demonstrated a stronger positive correlation with the MIB-1 index than that of ^{201}Tl. With the use of MIBI SPECT, we can estimate the proliferative activity of glioma noninvasively.

Keywords ^{99m}Tc-MIBI · ^{201}Tl · Glioma · MIB-1 · Proliferative activity

Introduction

Proliferative activity is an important prognostic factor in glioma [1, 2, 3, 4, 5]. Proliferation can be assessed by the detection of Ki-67, which is a nuclear antigen present in all parts of the cell cycle except for the G_0 phase. Conventionally, it is diagnosed immunohistopathologically using a monoclonal antibody for the Ki-67 antigen [1, 3, 4, 5, 6, 7, 8]. Because monoclonal antibody to Ki-67 antigen (MIB-1) shows higher affinity for Ki-67 than the previously generated MoAb [9, 10, 11], it has achieved widespread use, and MIB-1 proliferation indices are now assessed routinely in many neuropathology laboratories [1, 3, 4, 5, 6, 7, 8, 9, 10, 11].

Table 1 Tc-99m-MIBI, Tl-201 uptake parameters in comparison with MIB-1 index (*LGAS* low-grade astrocytoma, *ASA* anaplastic astrocytoma, *GBM* glioblastoma multiforme, *ER* early uptake ratio, *DR* delayed uptake ratio, *RI* retention index)

Case	Age (years)/ gender	Histology	MIBI			^{201}TI			MIB-1 (%)
			ER	DR	RI	ER	DR	RI	
1	14/M	LGAS	1.1	0.9	0.8	1.2	1.0	0.8	0.3
2	32/M	LGAS	1.1	1.4	1.2	1.7	1.5	0.9	0.0
3	39/F	LGAS	1.1	1.1	1.0	1.1	1.0	0.9	0.1
4	50/F	LGAS	0.9	1.2	1.3	1.0	1.1	1.1	1.8
5	57/M	LGAS	1.1	1.2	1.1	1.2	0.9	0.8	0.2
6	60/M	LGAS	1.7	1.5	0.9	1.1	1.2	1.0	0.3
7	32/M	ASA	3.4	4.4	1.3	2.7	3.0	1.1	7.3
8	37/M	ASA	4.0	4.0	1.0	3.7	3.7	1.0	2.3
9	53/F	ASA	12.3	13.3	1.1	2.9	4.8	1.6	30.0
10	55/M	ASA	1.8	1.9	1.0	4.9	5.1	1.0	0.9
11	82/F	ASA	7.0	6.5	0.9	3.5	3.8	1.1	6.8
12	43/M	GBM	6.9	7.3	1.1	3.6	5.6	1.5	29.0
13	46/M	GBM	10.8	9.9	0.9	3.4	4.2	1.2	37.0
14	48/F	GBM	6.9	4.9	0.7	2.8	3.6	1.3	15.0
15	53/M	GBM	2.2	1.6	0.8	1.5	1.7	1.1	15.0
16	55/M	GBM	9.8	11.4	1.2	6.5	8.8	1.3	25.0
17	56/M	GBM	6.5	7.2	1.1	4.0	5.0	1.3	15.4
18	61/M	GBM	5.9	4.8	0.8	2.7	4.6	1.7	15.0
19	68/M	GBM	5.0	4.2	0.8	2.9	3.0	1.0	12.1
20	68/M	GBM	4.5	4.3	0.9	1.6	1.7	1.1	3.0
21	69/M	GBM	2.5	2.6	1.0	1.7	3.0	1.8	10.8
22	69/M	GBM	2.5	3.4	1.3	1.8	2.0	1.1	26.8
23	72/M	GBM	6.4	7.9	1.2	3.2	4.1	1.3	17.9
24	73/M	GBM	12.2	16.0	1.3	4.2	5.7	1.4	17.0

Non-invasive measurement of tumor cell proliferation has been done using pyrimidine nucleus analogues, such as ^{11}C-thymidine or ^{131}I-iododeoxyuridine, to assess RNA and DNA [12, 13, 14, 15]. However, such unique radiopharmaceuticals are limited and restricted to specific institutes.

Alternatively, ^{201}Tl SPECT has been reported to be a non-invasive tool not only for the detection of a glioma but also for the prediction of both tumor type and histological grade [16, 17, 18]. Some investigators have reported a correlation between ^{201}Tl uptake and proliferative activity [2, 8]. However, the supposition is still controversial [12]. In addition, the ^{201}Tl-SPECT image is relatively poor, due to lower energy and smaller doses.

Technetium-99m methoxy-isobutylisonitrile (MIBI) is also a tumor-seeking agent used as a substitute for ^{201}Tl for the scintigraphic detection of a variety of malignant neoplasms [19, 20, 21, 22, 23, 24, 25, 26, 27, 28]. Because of the advantage of its higher photon emissions, with clearer images and higher target-to-background ratios, it is now used for detecting brain tumors and for distinguishing high-grade from low-grade gliomas [22, 23, 24, 25, 27]. In addition, MIBI has the capability of diagnosing the presence of P-glycoprotein-mediated anticancer drug resistance [26, 27, 29]. However, there has been less research regarding the correlation between MIBI uptake and cell proliferation in gliomas.

The current study was designed to evaluate the relationship between MIBI uptake and proliferative activity as determined by the immunohistochemical MIB-1 staining method. By comparing the results with those of ^{201}Tl, we determined which tracer would be more appropriate for estimating proliferative activities.

Materials and methods

The study population consisted of 24 patients with glioma (18 men, six women; mean age 59.4 ± 12.9 years, age range 32 to 77 years). Gliomas were further classified into low-grade astrocytomas (LGASs; grade I and II lesions) and high-grade or malignant gliomas including anaplastic astrocytomas (ASAs; grade III) and glioblastoma multiforme (GBM; grade IV). Taking into account the resolution of our SPECT device, we included in the study only patients with lesions greater than 2 cm maximum diameter on MRI. All patients entered a study protocol approved by the institutional review board (Table 1).

Scintigraphic technique

Dual SPECT scans were obtained at both 10 min (early) and 3 h (delayed) after simultaneous intravenous injections of 600 MBq of MIBI and 111 MBq of ^{201}Tl. Images were obtained by a dual isotope technique as previously reported [20, 21, 27]. Sixty-four projections of 40 s each were acquired by a triple-head gamma camera system with low-energy, high-resolution, and fan-beam collimators (Picker, Prism 3000). Three energy windows were used for

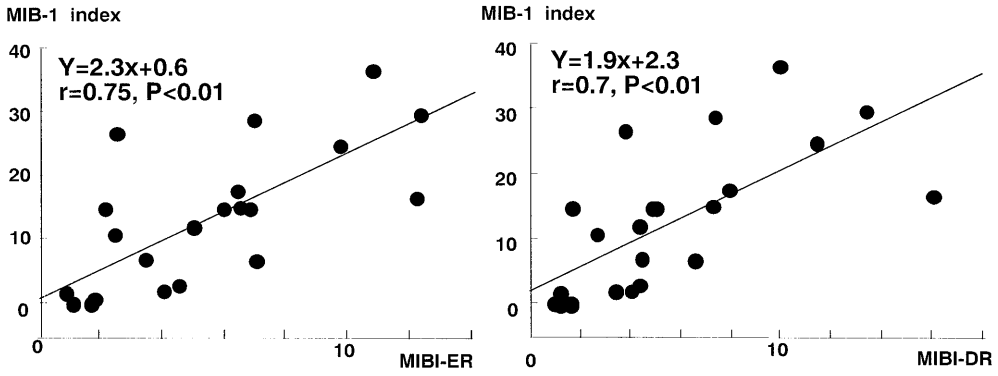

Fig. 1 Correlation between MIB-1 index and MIBI uptake ratio

acquisition; they were set at 72 keV with a 15% window for ^{201}Tl images, 90 keV with a 10% window for scatter images, and 141 keV with a 15% window for ^{99m}Tc images. These projection data were processed with a two-dimensional low-pass filter and then corrected for the contamination scatter. Image reconstruction was done by filtered back projection with a ramp filter.

Semi-quantitative analysis

We analyzed SPECT images using MR coronal images for anatomical guidance. A region of interest (ROI) was placed on a coronal slice with maximum lesion uptake. A manual ROI was traced around the lesion, and a round-shaped ROI with a 10-mm diameter was drawn on the opposite side in the appropriate location as a normal tissue. For each image set, early and delayed, an uptake ratio was calculated as follows:

$$\frac{(\text{Average counts in the lesion ROI})}{(\text{Average counts in the normal ROI})}$$

A retention index was also calculated [21, 27] as follows:

delayed uptake ratio/early uptake ratio

The current study involved simultaneous dual-isotope imaging, and the raw data at the 72-keV window were thus contaminated by ^{99m}Tc Compton scatter. In addition, the raw data at the 141-keV window included a gamma-ray count of ^{201}Tl. To eliminate this scatter contamination, we corrected the raw data on a pixel-by-pixel bias [20, 21, 27]. We set three kinds of energy windows, 72 keV, 90 keV, and 141 keV, for data collection. From phantom studies, the rate of scatter from the 141-keV in the 90-keV window was 1.06 times that of the 72-keV window. The correction data, therefore, can be obtained by the formula $a = A - \alpha C$, where A stands for the raw counts in the 72-keV window, C indicates the raw counts in the 90-keV window, and α is the scatter correction coefficient measured to be 1.06 [20, 21, 27]. Similarly, the cross-talk correction coefficient, β, was measured to be 0.22 [20, 21, 27], and corrected counts in the 141-keV window for the ^{99m}Tc image, b, were calculated by the formula $b = B - \beta a$, where B stands for the raw counts in the 141-keV window.

Immunohistochemistry

All patients underwent subsequent surgical excision of their tumors. Hematoxylin-eosin-stained sections were used to identify tumor areas for immunohistochemistry.

After deparaffinization and dehydration, the sections were microwaved in a citrate buffer for 10 min. The staining regimen was performed at room temperature and consisted of exposure to hydrogen peroxide and a blocking antibody to reduce background staining, followed by incubation with the primary monoclonal antibodies MIB-1 (Immunotech S.A., Marseilles, France), which recognizes an epitope of the Ki-67 antigen. The primary antibody was visualized with a biotinylated secondary antibody, the avidin-biotinylated enzyme complex, and a chromogen, diaminobenzidine. Hematoxylin was used as a counterstain. Each step was separated by a wash with a citrate buffer. Positive controls consisted of a tonsil section, while the primary antibody was replaced with a buffer in negative controls.

Using a high-power field (× 400), we counted nuclear stained cells. The MIB-1 index (MI) was obtained as the percentage of immunopositive cells from the total cells counted in the visualized fields of a given section. The number of MIB-1-positive cells per 100 tumor cells was designated as the MI and was also calculated in at least 1,000 cells.

Statistical analysis

To determine the correlation between the MI and SPECT parameters, we calculated Spearman' s rank correlation coefficient. A P value of < 0.05 was considered to be significant. Statistical analysis was performed with StatView version 5 (SAS Institute).

Results

All patients with ASAs and GBM showed an intense uptake of both radiopharmaceuticals. In most of the GBMs, the MI was higher than 10.0. Although the ASAs showed a variable MIB-1 value, most of them were lower than 10.0. Conversely, all LGASs showed faint or no uptake, and all MIs were lower than 0.5 (Table 1). A linear positive correlation was noted between the ER of the MIBI and MI ($r = 0.75$, $P < 0.01$). The DR of the MIBI also showed significant linear correlation ($r = 0.7$, $P < 0.01$) (Fig. 1).

As regards ^{201}Tl, there was a weak positive correlation between the DR ($r = 0.6$, $P < 0.01$) and the MI. However, no significant correlation was noted between the ER and MIs (Fig. 2). In contrast to the no-significant

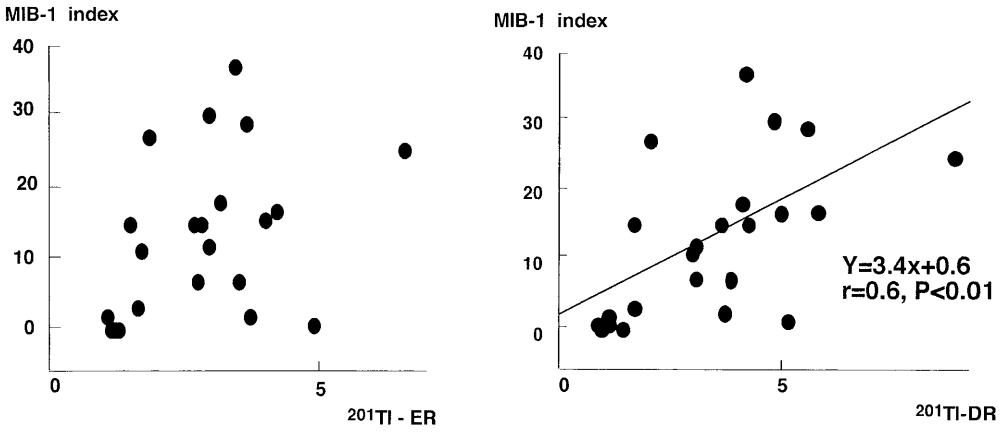

Fig. 2 Correlation between MIB-1 index and ^{201}Tl uptake ratio

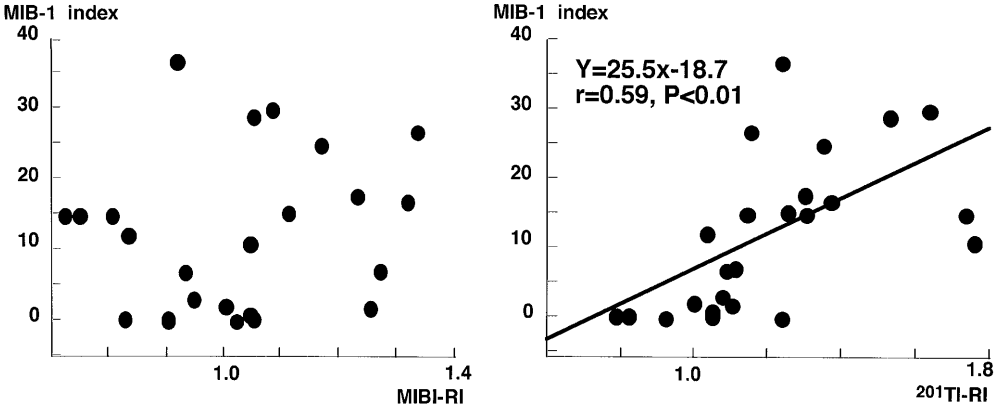

Fig. 3 Correlation between MIB-1 index and retention index

correlation between the RI and MIs in MIBI, the RI of ^{201}Tl correlated weakly (r = 0.59, $P < 0.01$) with the MI (Fig. 3).

Case presentation

Case 1 (case number 13) was a 46-year-old man with GBM. A Gd-enhanced T1-weighted MRI image revealed an irregularly shaped mixed-component tumor in the right temporal lobe. A prominent uptake of both radiopharmaceuticals within the tumor was noted. Uptake indices (ER, DR, and RI) of MIBI were 10.8, 9.9, and 0.9, respectively. The ^{201}Tl uptake indices were 3.4, 4.2, and 1.2, respectively. Immunostaining with monoclonal antibodies MIB-1 demonstrated numerous MIB-1-positive cells. The MI was 37 % (Fig. 4).

Case 2 (case number 11) was an 82-year-old woman with ASA. A Gd-enhanced T1-weighted MRI image showed a uniform ring-enhanced tumor in the right frontal lobe. Both the ^{201}Tl and the MIBI demonstrated intense uptake in accordance with the tumor. The ER, DR, and RI were 7.0, 6.5, and 0.9, respectively, in the MIBI, and 3.5, 3.8, and 1.1, respectively, in the ^{201}Tl. The MI was 6.8 % (Fig. 5).

Case 3 (case number 4) was a 50-year-old man with LGAS. The post-contrast T1-weighted MRI image showed a poorly enhanced tumor in the right frontal lobe. Neither MIBI nor ^{201}Tl uptakes were noted in the tumor. The ER, DR, and RI were 0.9, 1.2, and 1.3, respectively, in the MIBI, and 1.0, 1.1, and 1.1, respectively, in the ^{201}Tl. The specimen sections showed few positive immunostaining cells for MIB-1. The MI was 1.8 % (Fig. 6).

Discussion

A quantitative assessment of the proliferative potentials in a glioma provides direct knowledge about its biological behavior and aids in the finding of an accurate prognosis [1, 3]. Although mitotic figures are a conventional cellular proliferation index, they are variable in number in lower-grade tumors, and may even be difficult to find in small biopsies of high-grade tumors [3]. Proliferative activities, therefore, could not be estimated on routine

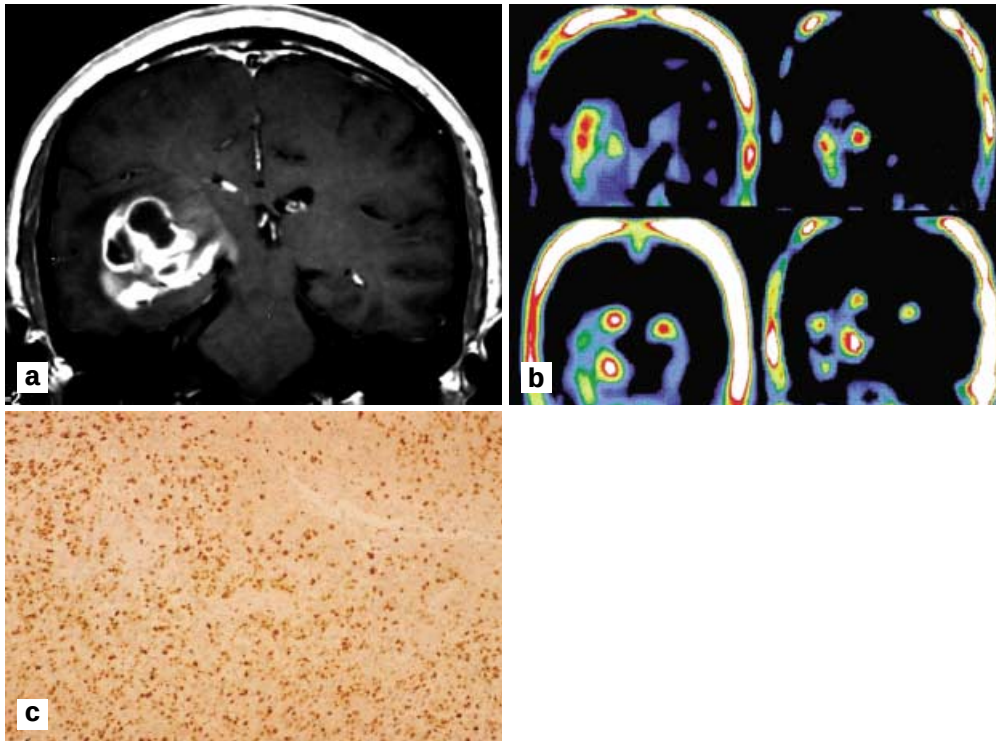

Fig. 4 a–c Case 13. A 46-year-old man with GBM. **a** A post-contrast T1-weighted image revealed an irregularly shaped mixed-component tumor in the right temporal lobe. **b** Both MIBI and ^{201}Tl accumulated prominently, coinciding with the tumor. The ^{201}Tl uptake is noted mainly in a lateral site (*left upper:* early; *right upper:* delayed). Conversely, MIBI accumulated dominantly in the medial site of the tumor (*left lower:* early; *right lower:* delayed). ER, DR, and RI of MIBI were 10.8, 9.9, and 0,9, respectively. The ^{201}Tl uptake indices were 3.4, 4.2, and 1.2, respectively. **c** Immunostaining of paraffin sections with a monoclonal antibody MIB-1 (× 40) showed numerous MIB-1-positive cells, and the MIB-1 index was 37 %

light-microscopic histopathological assessment [3]. Recently, cell proliferation activity has come to be estimated by immunohistochemical staining methods using the monoclonal antibody Ki-67 [1, 3, 4, 5, 6, 7, 8, 9, 10, 11]. The antigen is present throughout the G_1, S, G_2, and M phases in human cells, but it is absent in the G_0 phase. MIB-1, a monoclonal antibody, was recently used against recombinant parts of the Ki-67 antigen, which can be regarded as a "true" Ki-67 equivalent reactive with a nuclear antigen in paraffin-embedded materials. However, the evaluation of such proliferation markers with immunohistochemical preparations generally involves time-consuming and tedious cell counting by microscopy, which prevents the routine application of proliferation markers as diagnostic parameters in most laboratories. Such backgrounds demand convenient methods for the estimation of proliferative activity.

Previously, Oriuchi et al. reported a positive correlation between ^{201}Tl uptake and proliferation activity estimated by BUdR [2] and directed the potentiality of ^{201}Tl as an effective medium for characterizing tumor proliferation [2]. Nonetheless, the current study emphasized that MIBI uptake indices showed a more significant correlation with the MIs than with those of ^{201}Tl. Although the authors have no obvious explanation for the weaker correlation with MIB-1 observed with ^{201}Tl, several points were considered. Among them is the discordance of the uptake mechanism between each tracer except for the permeability of the blood–brain barrier. In the uptake of MIBI, strongly negative plasma-membrane potentials within the cells resulting from increased cellular metabolism contribute to uptake [30, 31, 32]. In addition, P-glycoprotein plays an important role, particularly, on delayed imaging [22]. Conversely, ^{201}Tl is taken up by two or more active transport systems such as the Na^+-K^+ ATPase membrane-pumping system [16, 17, 18]. Another factor is the difference in intratumoral distribution. Whereas only a small amount of ^{201}Tl accumulates inside the mitochondria, the majority of MIBI has an intramitochondrial location [30]. Previously, O'Tuama et al. reported that some LGASs could be detected with ^{201}Tl, but they could not be detected with MIBI [25]. Although such a noticeable discrepancy was not noted in the current study, certain differences should exist on histological levels, which would explain a stronger correlation between the MIBI uptake and the MI.

Another consequential factor is the difference in the referencing method used to measure the proliferative activity. BUdR is specifically incorporated into the DNA synthetic phase (S-phase) of the cell cycle, and that predicts only the S-phase fraction [12, 13, 14]. In contrast, the MIB-1 staining method covered not only the S-phase but also the G_1, G_2, and M stages that are also associated with proliferation during a cell's cycle of division. In addition, the derivation of a pyrimidine nucleoside such as BUdR to a tumor cell is limited by the presence of a blood–tumor barrier [12]. Such dissimilarities of referencing methods for cell proliferation

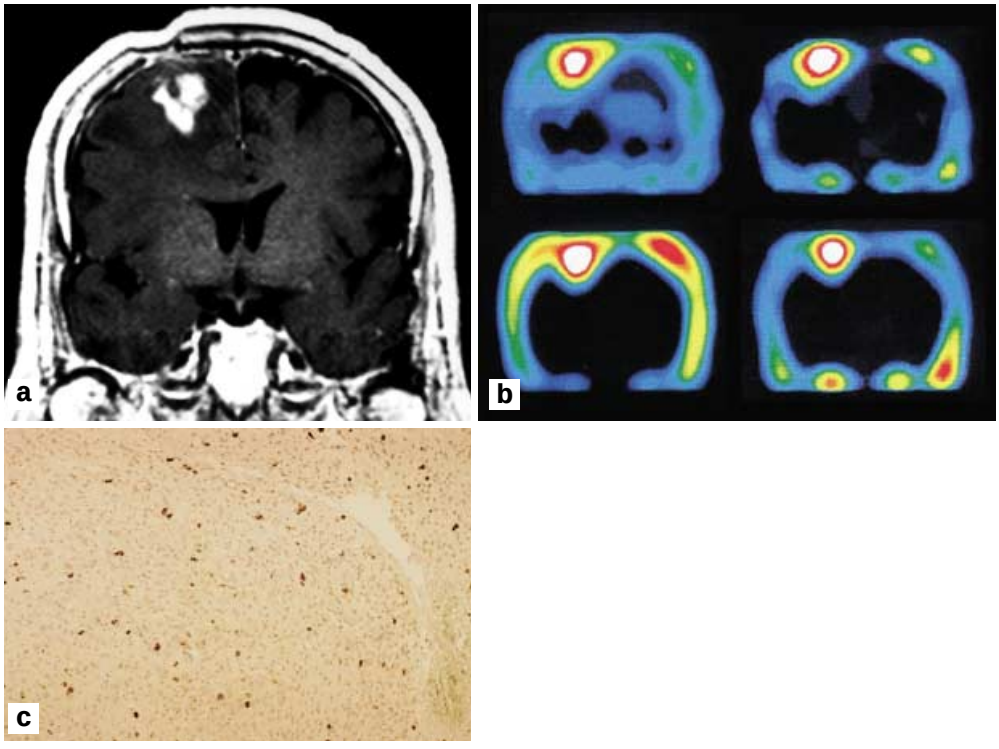

Fig. 5a–c Case 11. An 82-year-old woman with ASA. **a** A post-contrast T1-weighted image showed a uniform ring-enhanced tumor in the right frontal lobe. **b** Both ^{201}Tl and MIBI demonstrated an intense uptake in accordance with the tumor (*left upper:* early ^{201}Tl; *right upper:* delayed ^{201}Tl; *left lower:* early MIBI; *right lower:* delayed MIBI). The ER, DR, and RI were 3.5, 3.8, and 1.1, respectively, in the ^{201}Tl and 7.0, 6.5, and 0.9, respectively, in the MIBI. **c** Several positive cells are observed after MIB-1 staining. The MIB-1 index was 6.8 %

could be responsible for the difference between our data and those previously reported by other institutes [2]. The correlation coefficient improved in ^{201}Tl on the delayed images because of the serial change of tracer distribution probably due to the phenomenon that ^{201}Tl was retained in mainly active or viable tumor cells. As the value of the RI also reflects a washout phase, the RI of ^{201}Tl is also correlated with MIB-1. In contrast, the distribution of most MIBI remained unchanged on the delayed image, particularly in GBM. Because our previous research demonstrated that GBM contained few P-glycoproteins (P-gps) [22, 27], an enhanced washout phenomenon did not occur. Therefore, the RI of MIBI has no meaning in such conditions. In practical use, we can estimate the proliferative activity during the early image of MIBI without consuming a lot of time, which is one of the advantages of MIBI.

These results lead to an important clinical implication about therapeutic strategy, namely, that intense and repeated chemotherapy should be recommended in the treatment of GBM because of its high proliferative activity. However, in choosing anticancer drugs, drug resistance related to P-gp may not be taken into account. In contrast, it is difficult to choose an anticancer drug in LGAS. Because of low proliferative activity, intense anticancer chemotherapy may be unnecessary. Nevertheless, when chemotherapy is performed, the use of anticancer drugs with multidrug resistance related to P-gp should be avoided.

The other clinical implication addressed in the current study is prognostic value. Although the malignant biological behavior of neoplasm is determined by many factors [33, 34, 35], the proliferative potential is the strongest prognostic factor for predicting patient survival [1]. We previously reported that intense MIBI uptake could predict a poor clinical outcome in GBM [27]. The enhanced proliferative activity may explain the result.

Recently, [^{18}F]-FDG has come to be used widely to identify the malignancy grade of lesions and to monitor therapeutic outcome [17, 36], but it does not correlate with the proliferative rate [37]. Further studies, however, are necessary to assess the clinical relevance. A combined use of [^{18}F]-FDG with MIBI could be a promising method for the detection of the characteristics of a glioma, including metabolism and proliferation.

An inevitable study limitation is that tissue sampling is usually performed by referencing the findings of light microscopic examinations, which do not provide direct information about biological behaviors. In addition, viable cells are not always distributed homogeneously in tumor tissue [7]. The possibility of cyclical mitotic activity is also present in immunohistochemical analysis. Such a sampling error and the limitations of the number of sampling specimens might also affect the result.

The other limitation is the ROI setting. Although we traced the ROIs under the reference of MRI, they did not always accord with tumor contour correctly. In particular, a tumor with low tracer uptake, such as LGAS,

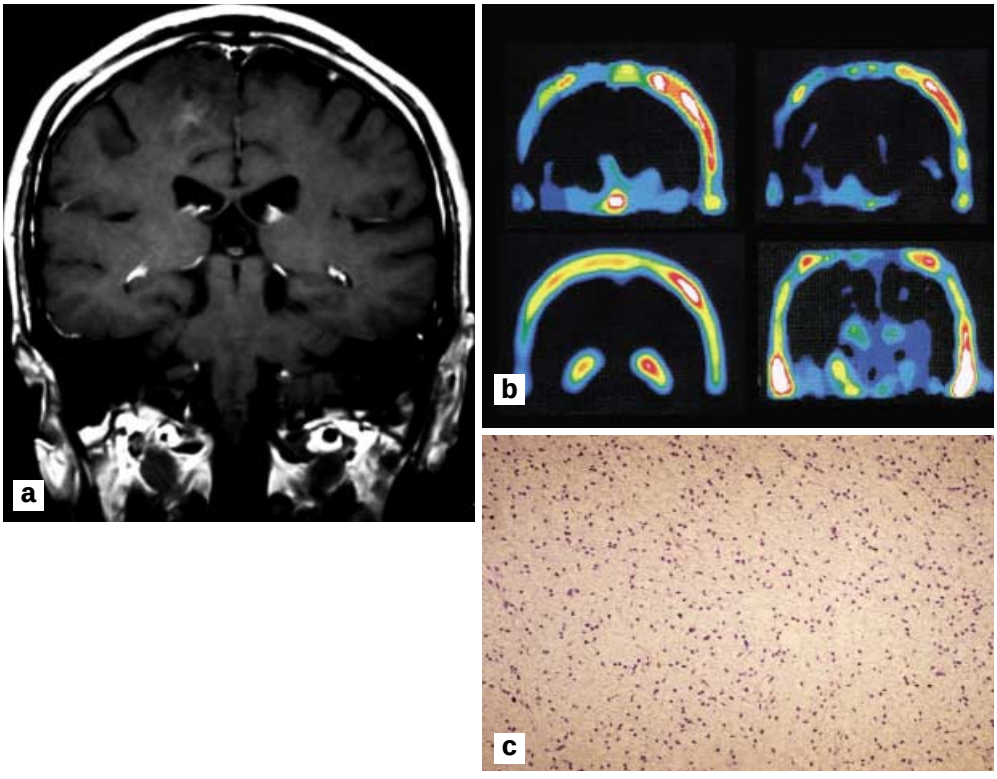

Fig. 6 a–c Case 4. A 50-year-old man with LGAS. **a** A post-contrast T1-weighted image showed a poorly enhanced tumor in the right frontal lobe. **b** Neither MIBI nor ^{201}Tl uptakes were noted in the tumor (*left upper:* early ^{201}Tl; *right upper:* delayed ^{201}Tl; *left lower:* early MIBI; *right lower:* delayed MIBI). The ER, DR, and RI were 1.0, 1.1, and 1.1, respectively, in the ^{201}Tl and 0.9, 1.2, and 1.3, respectively, in the MIBI. **c** The specimen sections showed no positive immunostaining cells for MIB-1. The MIB-1 index was 1.8 %

is difficult for ROI tracing. To overcome this drawback, combined CT/SPECT tomography has come to be used [38]. However, it is still available at only a limited number of institutes and requires special equipment and software. In the future, such dual-modality devices will be widely used and will make the study more reliable.

In conclusion, compared with ^{201}Tl, the degree of MIBI uptake was considered to be more closely related to proliferative activity in glioma. Previously, some advantages of MIBI over ^{201}Tl, such as its imaging quality [25] and its being a substrate for P-glycoprotein [26, 27], had been reported. The current study added another meaningful advantage for MIBI, namely, its being a clinical marker for the proliferative activity in glioma.

References

1. Wakimoto H, Aoyagi M, Nakayama T, Nagashima G, Yamamoto S, Tamaki M, Hirakawa K (1996) Prognostic significance of Ki-67 labeling indices obtained using MIB-1 monoclonal antibody in patients with supratentorial astrocytomas. Cancer 77: 373–380
2. Oriuchi N, Tamura M, Shibazaki T, et al. (1993) Clinical evaluation of thallium-201 SPECT in supratentorial gliomas: relationship to histologic grade, prognosis and proliferative activities. J Nucl Med 34: 2085–2089
3. Rachamimov AOS, Louis DN (1997) Histopathologic and immunohistochemical prognostic factors in malignant gliomas. Curr Opin Oncol 9: 230–234
4. Kirkegaard LJ, DeRose PB, Yao B, Cohen C (1998) Image cytometric measurement of nuclear proliferation markers (MIB-1, PCNA) in astrocytomas. Prognostic significance. Am J Clin Pathol 109: 69–74
5. Nishizaki, Harada K, Kajiwara K, Nakayama H, Ito H (1998) Proliferative potentials of glioma cells and vascular components determined with monoclonal antibody MIB-1. J Exp Clin Cancer Res 16: 153–157
6. Schiffer D, Cavalla P, Dutto A, Borsotti L (1997) Cell proliferation and invasion in malignant gliomas. Anticancer Res 17: 61–69
7. Ide M, Jimbo M, Yamamoto M, Kubo O (1997) Tumor cell counting using an image analysis program for MIB-1 immunohistochemistry. Neurol Med Chir 37: 158–162
8. Ishibashi M, Taguchi A, Sugita Y, Morita S, Kawamura S, Umezaki N, et al. (1995) Thallium-201 in brain tumors: Relationship between tumor cell activity in astrocytic tumor and proliferating cell nuclear antigen. J Nucl Med 36: 2201–2206
9. Gerdes J, Becker MHG, Key G, Gattoretti G (1992) Immunohistological detection of tumor growth fraction (Ki-67 antigen) in formalin-fixed and routinely processed tissues. J Pathol 168: 85–86

10. Nagashima G, Aoyagi M, Wakimoto H, Tamaki M, Ohno K, Hirakawa K, et al. (1995) Immunohistochemical detection of progesterone receptors and the correlation with the Ki-67 labeling indices in paraffin-embedded sections of meningiomas. Neurosurgery 37: 478–483
11. Onda K, Davis RL, Shibuya M, Wilson CB, Hoshino T (1994) Correlation between the bromodeoxyuridine labeling index and the MIB-1 and Ki-67 proliferating cell indices in cerebral glioma. Cancer 74: 1921–1926
12. Tjuvajev JG, Macapinlac HA, Daghighian F, Scott AM, Ginos JZ, Finn RD, et al. (1994) Imaging of brain tumor proliferative activity with iodine-131-iododeoxyuridine. J Nucl Med 35: 1407–1417
13. Borght TV, Pauwel S, Lambotte L, Labar D, Maeght De, Stroobandt G, et al. (1994) Brain tumor imaging with PET and 2-[Carbon-11] thymidine. J Nucl Med 35: 974–982
14. Schmidtke RS, Rüth F, Bernatz S (1999) Radiolabeled thymidine: a sensitive tracer for early tumor response and recurrence after irradiation. J Nucl Med 40: 1702–1705
15. Goethals P, Lameire N, van Eijkeren M, Kosteloot D, Thierens H, Dams R (1996) (Methyl-carbon-11) thymidine for in vivo measurements of cell proliferation. J Nucl Med 37: 1048–1052
16. Kaplan WD, Takvorian T, Morris JH, et al. (1987) Thallium-201 brain tumor imaging: a comparative study with pathologic correlation. J Nucl Med 28: 47–52
17. Tamura M, Shibasaki T, Zama A, Kurihara H, Horikoshi S, Ono N, et al. (1998) Assessment of malignancy of glioma by positron emission tomography with ^{18}F-fluorodeoxyglucose and single photon emission computed tomography with thallium-201 chloride. Neurosurgery 40: 210–215
18. Ueda T, Kaji Y, Wakisaka S, Watanabe K, Hoshi H, Jinnouchi S, et al. (1993) Time sequential SPET studies in brain tumor using ^{201}Tl. Eur J Nucl Med 20: 138–145
19. Abdel-Dayem HM, Scott AM, Macapinlac HA, El-Gazzar AH, Larson SM (1994) Role of ^{201}Tl-chloride and ^{99m}Tc sestamibi in tumor imaging. In: Freeman LM (ed) Nuclear Medicine Annual. Raven Press, New York, pp181–234
20. Nishiyama Y, Kawasaki Y, Yamamoto Y, Fukunaga K, Satoh K, Takashima H, et al. (1997) Technetium-99m-MIBI and thallium-201 scintigraphy of primary lung cancer. J Nucl Med 38: 1358–1361
21. Nagamachi S, Jinnouchi S, Flores LG, Ohnishi T, Nakahara H, Futami S. et al. (1997) Evaluation of primary lung cancer and mediastinal lymph node metastasis using ^{99m}Tc-MIBI: comparison with ^{201}Tl and relation to chemotherapeutic effect. Kakuigaku 34: 453–463
22. Nagamachi S, Jinnouchi S, Flores LG II, Kodama T, Ohnishi T, Nakahara H, et al. (1998) Evaluation of brain tumor by ^{99m}Tc-MIBI: comparison study with ^{201}Tl and predictivity of therapeutic effect. Kakuigaku 35: 121–130
23. Baillet G, Albuquerque L, Chen Q, et al. (1994) Evaluation of single-photon emission tomography imaging of supratentorial brain gliomas with technetium-99m sestamibi. Eur J Nucl Med 21: 1061–1066
24. Bagni B, Pinna L, Tamarroz R, Cattaruzzi E, Marzola MC, Bagni I, et al (1995) SPET imaging of intracranial tumors with ^{99m}Tc-sestamibi. Nucl Med Commun 16: 258–264
25. O'Tuama LA, Treves ST, Larar JN, Packard AB, Kwan AJ, Barnes PD, et al. (1993) Thallium-201 versus technetium-99m-MIBI SPECT in evaluation of childhood brain tumors: a within-subject comparison. J Nucl Med 34: 1045–1051
26. Andrews DW, Das R, Kim S, Zhang J, Curtis M (1997) Technetium-MIBI as a glioma imaging agent for the assessment of multi-drug resistance. Neurosurgery 40: 1323–1344
27. Nagamachi S, Jinnouchi S, Ohnishi T, Nakahara H, Leo G Flores II, Tamura S, et al. (1999) The usefulness of ^{99m}Tc-MIBI for evaluating brain tumors: comparative study with ^{201}Tl and relation with P-glycoprotein. Clin Nucl Med 24: 765–772
28. Maffioli L, Gasparini M, Chiti A, Gramaglia A, Mongioj V, Pozzi A, et al. (1996) Clinical role of technetium-99m sestamibi single-photon emission tomography in evaluating pretreated patients with brain tumors. Eur J Nucl Med 23: 308–311
29. Piwnica WD, Chiu ML, Budding M, Kronauge JF, Kramer RA, Croop JM (1993) Functional imaging of multidrug-resistant P-glycoprotein with an organotechnetium complex. Cancer Res 53: 977–984
30. Arbab AS, Koizumi K, Toyama K, et al. (1997) Ion transport systems in the uptake of ^{99m}Tc-tetrofosmin, ^{99m}Tc-MIBI and ^{201}Tl in a tumor cell line. Nucl Med Commun 18: 235–240
31. Chen LB (1988) Mitochondrial membrane potential in living cells. Annu Rev Cell Biol 4: 155–181
32. Arbab AS, Koizumi K, Toyama K, Araki T (1996) Uptake of technetium-99m-tetrofosmin, technetium-99m-MIBI and thallium-201 in tumor cell lines. J Nucl Med 37: 1551–1556
33. Ritter AM, Sawaya R, Hess KR, Levin VA, Bruner JM (1994) Prognostic significance of bromodeoxyuridine labeling in primary and recurrent glioblastoma multiforme. Neurosurgery 35: 192–198
34. Nagano N, Sasaki H, Aoyagi M, Hirakawa K (1993) Invasion of experimental rat brain tumor: early morphological changes following microinjection of C6 glioma cells. Acta Neuropathol 86: 117–125
35. Takamiya Y, Brem H, Ojeifo J, Minera T, Martuza RL (1994) AGM-1470 inhibits the growth of human glioblastoma cells in vitro and in vivo. Neurosurgery 34: 869–875
36. Sasaki M, Kuwabara Y, Yoshida T, Nakagawa M, Fukumura T, Mihara F, et al. (1998) A comparative study of thallium-201 SPET, carbon-11 methionine PET and fluorine-18 fluorodeoxyglucose PET for the differentiation of astrocytic tumors. Eur J Nucl Med 25: 1261–1269
37. Higashi K, Clavo AC, Wahl RL (1993) Does FDG uptake measure proliferative activity of human cancer cells? In vivo comparison with DNA flow cytometry and tritiated thymidine uptake. J Nucl Med 34: 414–419
38. Thurfjell L, Lau YH, Andersson JLR, Hutton BF (2000) Improved efficiency for MRI-SPET registration based on mutual information. Eur J Nucl Med 27: 847–856